Pauli principle and chaos in a magnetized disk

R. Badrinarayanan,[1] A. Góngora-T,[2] and Jorge V. José[1]
[1]*Physics Department and Center for Interdisciplinary Research on Complex Systems, Northeastern University, Boston, Massachusetts 02115*
[2]*Centro de Ciencias Físicas, Universidad Nacional Autónoma de México, Apartado Postal 48-3, 62250 Cuernavaca, Morelos, Mexico*
(Received 28 December 1998)

We present results of a detailed quantum-mechanical study of a gas of N noninteracting electrons confined to a circular boundary and subject to homogeneous dc plus ac magnetic fields [$B=B_{dc}+B_{ac}f(t)$, with $f(t+2\pi/\omega_0)=f(t)$]. We earlier found a one-particle *classical* phase diagram of the (scaled) Larmor frequency $\tilde{\omega}_c=\omega_c/\omega_0$ vs $\epsilon=B_{ac}/B_{dc}$ that separates regular from chaotic regimes. We also showed that the quantum spectrum statistics changed from Poisson to Gaussian orthogonal ensembles in the transition from classically integrable to chaotic dynamics. Here we find that, as a function of N and $(\epsilon,\tilde{\omega}_c)$, there are clear quantum signatures in the magnetic response, when going from the single-particle classically regular to chaotic regimes. In the quasi-integrable regime the magnetization nonmonotonically oscillates between diamagnetic and paramagnetic as a function of N. We quantitatively understand this behavior from a perturbation theory analysis. In the chaotic regime, however, we find that the magnetization oscillates as a function of N but it is *always* diamagnetic. Equivalent results are also presented for the orbital currents. We also find that the time-averaged energy grows as N^2 in the quasi-integrable regime but changes to a linear N dependence in the chaotic regime. In contrast, the results with Bose statistics are akin to the single-particle case and thus different from the fermionic case. We also give an estimate of possible experimental parameters where our results may be seen in semiconductor quantum dot billiards. [S1063-651X(99)05208-3]

PACS number(s): 05.45.−a, 03.65.−w, 72.20.Ht

I. INTRODUCTION

There is a long history of studies of the magnetic response of an electron gas, confined to a finite boundary. Starting with Bohr and van Leeuwen [1], to Landau's finite diamagnetism in the quantum regime [2,3]. The problem is still of current theoretical an experimental interest [4], in particular due to the realization that for most geometries of the confining boundary one can find classically chaotic behavior [5–18]. Most previous studies of this problem have assumed that the external magnetic field is static and they have concentrated on calculating the static magnetic susceptibility, except for the dynamic magnetic field experimental work of Reulet *et al.* [19].

In an earlier paper [20] (referred to as I hereafter), we investigated the classical dynamics and the quantum signatures of classical chaos, for *one electron* confined to a circular quantum dot structure. The dot was subjected to uniform dc ($B_{\rm dc}$) plus ac ($B_{\rm ac}f(t)$), with periodic $f(t)=f(t+2\pi/\omega_0)$ perpendicular magnetic fields. There, we established an approximate phase boundary in the parameter space spanned by $(\epsilon=B_{ac}/B_{\rm dc},\tilde{\omega}_c=\omega_c/\omega_0)$ that separates the classically regular from the chaotic regimes, where ω_c is the Larmor frequency of the dc field. The phase diagram shown in Fig. 1, which we shall often use in our analysis here, separates the quasi-integrable from chaotic regimes. In I we established clear correspondences between the transitions in the classical behavior and their corresponding quantum signatures. From identifying the statistical properties of the quasienergy spectrum of the one-period evolution operator, going from Poisson (integrable) to Gaussian orthogonal ensemble (chaotic), to the semiclassical phase space correspondence, Husimi quasienergy eigenfunction distribution functions.

In this paper we present a detailed quantum-mechanical study of the zero temperature magnetic response of a noninteracting electron gas confined to a circular boundary and subject to the same combination of a dc plus ac magnetic fields. Here we are interested in considering the magnetic response of this model for an N electron system that satisfies the Pauli exclusion principle. Another basic question, first addressed in this paper, is how does the transition from regular to chaotic behavior in the classical case, where the particles are indistinguishable, affect their fermionic quantum nature. Most previous studies of the quantum manifestations

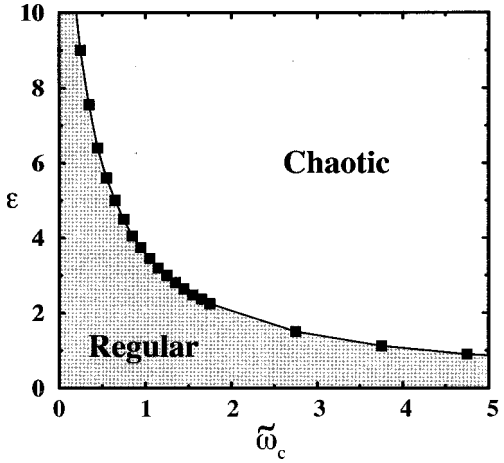

FIG. 1. Classical phase diagram separating the regular from chaotic regions used in the analysis of this paper. See the text for the definition of the dimensionless variables in the axes.

of classical chaos have centered on one-particle problems. Here we only address the important particle-statistics many-particle problem, and leave for a future study the relevant effects of electronic interactions. As we show below, there are indeed clear manifestations of the particle statistics, which are different if we are in the classically integrable regime from those where the system is chaotic.

The organization of the rest of the paper is as follows. In Sec. II we briefly recapitulate the main elements of the single particle model studied in I, together with expressions for the matrix elements of the operators needed in our analysis. Next we outline our method to calculate the matrix elements of multi-electron operators in a basis of properly (anti)symmetrized eigenfunctions. In Sec. III we present our main results for the magnetization, orbital currents, and energy. We calculated both the time evolution of such operators and their time averages as a function N and the parameters $(\epsilon, \tilde{\omega}_c)$. We also include a perturbative calculation, fully described in the Appendix, that quantitatively explains our numerical results for the magnetization in the quasi-integrable weak-field regime. Finally, in Sec. IV we present a summary of our conclusions, with an estimate of a few experimental parameters that may give an idea of the regimes in frequency and fields where the transition between integrable and chaotic regimes discussed in this paper could be tested.

II. THE MODEL

A. One-electron wave function

We start by recalling the main features of the single particle formalism, as explained in paper I, and next its extension to the N noninteracting electron problem. The model we consider here is that of electrons confined to a disk, and subject to a steady ($B_{\rm dc}$) and a time-periodic ($B_{\rm ac}$) magnetic field. After scaling to appropriate dimensionless units, the model Hamiltonian considered here is

$$\tilde{H} = \tilde{H}_{\rm dc} + \tilde{H}_1(\tau), \tag{1}$$

which in polar coordinates reads

$$\tilde{H}_{\rm dc} = -\frac{\tilde{\hbar}^2}{2}\left(\frac{d^2}{dr^2} + \frac{1}{r}\frac{d}{dr}\right) + \frac{\ell^2\tilde{\hbar}^2}{2r^2} + \frac{1}{2}\left(\frac{\tilde{\omega}_c}{2}\right)^2 r^2 + \ell\tilde{\hbar}\frac{\tilde{\omega}_c}{2}, \tag{2}$$

and with the time-dependent kick component

$$\tilde{H}_1(\tau) = \frac{1}{2}\ \eta\ r^2 \sum_{n=-\infty}^{\infty} \delta(\tau - n). \tag{3}$$

The dimensionless units are defined as

$$r = \frac{\rho}{R_0},\ \ 0 \leqslant r \leqslant 1,\ \ \tau = \frac{t}{T_0} \equiv \frac{\omega_0}{2\pi}t, \tag{4}$$

$$\tilde{\omega}_c = \frac{\omega_c}{\omega_0},\ \ \tilde{\hbar} = \frac{\hbar}{m^*\omega_0 R_0^2},\ \ \epsilon = \frac{B_{\rm ac}}{B_{\rm dc}} = \frac{\omega_{\rm ac}}{\omega_c},\ \ \text{and}\ \ \eta = \left(\frac{\epsilon\,\tilde{\omega}_c}{2}\right)^2. \tag{5}$$

Here R_0 is the radius of the disk quantum dot assumed to have rigid walls. T_0 is the drive period of the ac field, $\omega_c = e^*B_{\rm dc}/(m^*c)$ is the static Larmor frequency, in terms of the effective electron mass m^* ($\sim 0.067 m_e$), the screened electronic charge e^* ($\sim 0.3e$) [21], and the dynamic frequency $\omega_{\rm ac} = e^*B_{\rm ac}/(m^*c)$.

The exact eigenfunctions of the static Hamiltonian $\tilde{H}_{\rm dc}$ are given in terms of the Whittaker M functions [3]

$$\tilde{\psi}_{n\ell}(r) = \sqrt{\frac{2}{N_{n\ell}}}\ \frac{1}{r} M_{\chi_{n\ell},|\ell|/2}\left(\frac{f}{2}r^2\right), \tag{6}$$

with n the principal quantum number, ℓ the angular momentum eigenvalue, and $N_{n\ell}$ a normalization constant. The frustration parameter f that measures the number of flux quanta in the disk is defined by

$$f = \frac{\Phi}{\Phi_0} \equiv \frac{B_{\rm dc}\pi R_0^2}{(hc/2e^*)} \equiv \frac{\tilde{\omega}_c}{\tilde{\hbar}} = \left(\frac{R_0}{\ell_B}\right)^2, \tag{7}$$

with $\ell_B = (\hbar c/eB_{\rm dc})^{1/2}$ the magnetic length and $\Phi_0 = hc/2e^*$ the quantum of flux. The eigenenergies

$$\tilde{E}_{n\ell} = 2(\chi_{n\ell} + \ell) \tag{8}$$

are determined by the requirement that the wave function vanishes at the boundary, i.e., by the zeros of the Whittaker function $M_{\chi_{n\ell},|\ell|/2}(f/2) = 0$.

We calculated the energy eigenvalues $\tilde{E}_{n\ell}$ for the static problem in a basis of Whittaker functions as a function of $B_{\rm dc}$, and checked our numbers by fully reproducing the results of Ref. [5]. The Whittaker functions have the advantage of being valid over the entire range of parameters, however, they are numerically difficult to evaluate for the full time-dependent problem. For convenience when calculating the time-dependent problem, we decided also to expand the total (single particle) wave function in a Fourier-sine basis. In this case

$$\langle r|\tilde{H}_{\rm dc}|\tilde{\psi}_{n\ell}(\phi)\rangle = \tilde{E}_{n\ell}\,\tilde{\psi}_{n\ell}(r)\frac{e^{i\ell\phi}}{\sqrt{2\pi}}, \tag{9}$$

$$\langle r|\tilde{\Psi}(\phi)\rangle = \sum_{n=1}^{\infty}\sum_{\ell=-\infty}^{\infty}\tilde{\psi}_{n\ell}(r)\frac{e^{i\ell\phi}}{\sqrt{2\pi}}, \tag{10}$$

$$\tilde{\psi}_{n\ell}(r=1) = 0,\ \ \int_0^1 \tilde{\psi}_{n\ell}^2(r)\,r\,dr = 1, \tag{11}$$

$$\text{and}\ \ \langle r|\tilde{\psi}_{n\ell}\rangle = \sqrt{\frac{2}{r}}\sin(n\pi r). \tag{12}$$

This basis set is properly orthonormalized, and automatically satisfies the boundary conditions. To calculate the spectrum of the static problem, we used, nonetheless, the exact eigenvalues of $\tilde{H}_{\rm dc}$, given by the zeros of the Whittaker functions. Doing this allowed us also to check the reliability of our sine-basis numerical method.

We then computed the required matrix elements of the operators we are interested in, within the sine-basis method. For example, for the magnetization operator

$$\boldsymbol{\mu}=\frac{e^*}{2m^*c}\left(\boldsymbol{\mathcal{L}}-\frac{e^*}{c}\ \mathbf{r}\times\mathbf{A}(\mathbf{r})\right), \tag{13}$$

where $\boldsymbol{\mathcal{L}}$ is the angular momentum operator and $\mathbf{A}(\mathbf{r})$ is the electromagnetic vector potential in normalized coordinates. In the present case, we take the magnetic field perpendicular to the plane, then the z component of the magnetization operator is

$$\tilde{M}_z(r)=\frac{\hat{M}_z}{\mu_B}=-\frac{\hat{L}_z}{\tilde{\hbar}}-\frac{f}{2}\hat{r}^2, \tag{14}$$

with L_z the z component of the angular momentum, $\mu_B=|e^*|\hbar/2m^*c$ the Bohr magneton, and $\hat{M}_z$ the magnetization operator along the z axis. The matrix elements of $\tilde{M}_z$ in the Fourier sine basis are given by

$$\langle m|\tilde{M}_z|n\rangle=-\left\{\ell+\frac{f}{2}\left(\frac{1}{3}-\frac{1}{2n^2\pi^2}\right)\right\}\delta_{mn}-\left\{\frac{f}{2}\ \frac{(-)^{m+n}}{\pi^2}\frac{8mn}{(m^2-n^2)^2}\right\}(1-\delta_{mn}). \tag{15}$$

Similarly, starting from the definition of the current density operator

$$\mathbf{J}=\frac{1}{2m^*}\left(-i\hbar\boldsymbol{\nabla}-\frac{e^*}{c}\mathbf{A}\right)+\text{c.c.}, \tag{16}$$

(where c.c. stands for complex conjugate), we have the following expression for the azimuthal current densities: $J_\phi=J_\phi^{(\text{para})}+J_\phi^{(\text{dia})}$, where

$$J_\phi^{(\text{para})}=-\frac{i\tilde{\hbar}}{2}\frac{1}{r}\frac{\partial}{\partial\phi}+\text{c.c.}\ \text{ and }\ J_\phi^{(\text{dia})}=\frac{\tilde{\omega}_c}{2}r, \tag{17}$$

are the paramagnetic and diamagnetic current densities, respectively. In the Fourier-sine basis, the matrix elements of the current densities (in units of $\tilde{\hbar}$) are given by

$$\langle m|J_\phi^{(para)}|n\rangle=\ell\tilde{\hbar}\begin{cases}-\text{Ci}[2n\pi]+\gamma_E+\ln(2n\pi) & (m=n),\\ -\text{Ci}[(m+n)\pi]+\text{Ci}[(m-n)\pi] & (m\neq n),\end{cases} \tag{18}$$

$$\langle m|J_\phi^{(\text{dia})}|n\rangle=\frac{f}{2}\tilde{\hbar}\begin{cases}\frac{1}{2} & (m=n),\\ \frac{(-)^{m+n}-1}{\pi^2}\frac{4mn}{(m^2-n^2)^2} & (m\neq n),\end{cases} \tag{19}$$

where $\gamma_E=0.57721\ \ 566649,\ldots,$ is Euler's gamma number, and $\text{Ci}(x)$ is the cosine integral.

Finally, the expression for the one-period time-evolution operator $U_\ell(\tau,\tau_0)$, for the single particle Hamiltonian, which satisfies the dynamical equation

$$i\tilde{\hbar}\frac{\partial}{\partial\tau}U_\ell(\tau,\tau_0)=[\tilde{H}_{dc}+\tilde{H}_1(\tau)]U_\ell(\tau,\tau_0), \tag{20}$$

is

$$U_\ell(1,0)=\exp\left(-\frac{i}{\tilde{\hbar}}\frac{1}{2}\eta r^2\right)\exp\left(-\frac{i}{\tilde{\hbar}}\tilde{H}_{\text{dc}}\right). \tag{21}$$

The total (single particle) wave function at any integer multiple N_T of the period (hereafter taken to be 1), is given by repeated applications of U_ℓ to the initial wave function

$$|\Psi_\ell(r,\phi,N_T)\rangle=U_\ell^{N_T}|\Psi_\ell(r,\phi,0)\rangle. \tag{22}$$

B. Many-electron wave functions

One can directly generalize the above single-electron formalism to the many-electron case. Take the initial N-electron wave function to be

$$|\Phi(\boldsymbol{r}_1,\boldsymbol{r}_2,\ldots,\boldsymbol{r}_N)\rangle\equiv|\Phi(1,2\ldots,N)\rangle, \tag{23}$$

which is antisymmetric under exchange of an odd number of particles (the Pauli exclusion principle):

$$|\Phi(1,\ldots,i,\ldots,j,\ldots,N)\rangle=-|\Phi(1,\ldots,j,\ldots,i,\ldots,N)\rangle. \tag{24}$$

Let the ith single-particle eigenstate satisfy the equation

$$\tilde{H}^{(i)}|\Psi_{n_i\ell_i}(i)\rangle=E^{(i)}_{n_i\ell_i}|\Psi_{n_i\ell_i}(i)\rangle. \tag{25}$$

We know that the Slater antisymmetrization procedure for the noninteracting N-electron state can be written as the following tensor product [22]:

$$\hat{\mathbf{A}}|\Phi(1,2,\ldots,N)\rangle=\frac{1}{\sqrt{N!}}\begin{vmatrix} |\Psi_{n_1\ell_1}(1)\rangle & \otimes|\Psi_{n_2\ell_2}(1)\rangle & \cdots & \otimes|\Psi_{n_N\ell_N}(1)\rangle \\ |\Psi_{n_1\ell_1}(2)\rangle & \otimes|\Psi_{n_2\ell_2}(2)\rangle & \cdots & \otimes|\Psi_{n_N\ell_N}(2)\rangle \\ \vdots & \vdots & \ddots & \vdots \\ |\Psi_{n_1\ell_1}(N)\rangle & \otimes|\Psi_{n_2\ell_2}(N)\rangle & \cdots & \otimes|\Psi_{n_N\ell_N}(N)\rangle \end{vmatrix}$$

$$=\frac{1}{\sqrt{N!}}\sum_P \delta_P[|\Psi_{P\{n_1\ell_1\}}(1)\rangle\otimes|\Psi_{P\{n_2\ell_2\}}(2)\rangle\cdots\otimes|\Psi_{P\{n_N\ell_N\}}(N)\rangle], \tag{26}$$

where $\hat{\mathbf{A}}$ is the antisymmetrization operator and P is the permutation operator

$$P\{1,2,\ldots,N\}=\{P1,P2,\ldots,PN\}, \tag{27}$$

$$\delta_P=\begin{cases}+1 & (\text{even } P),\\ -1 & (\text{odd } P).\end{cases} \tag{28}$$

The summation runs over all possible permutations. Furthermore, the trace of any sum of N-body operators $\hat{O}=\Sigma_{i=1}^{N}\hat{O}_i$ can be written as

$$\mathrm{Tr}\{\hat{O}\}=\langle\Phi(1,\ldots,N)|\hat{O}|\Phi(1,\ldots,N)\rangle$$
$$=\frac{1}{N}\sum_{i,j=1}^{N}\langle\Psi_{n_i\ell_i}(j)|\hat{O}_j|\Psi_{n_i\ell_i}(j)\rangle. \tag{29}$$

Now consider the time evolution of such a system. For simplicity, we take as the initial state the lowest energy (ground) state of the *unperturbed* system (i.e., without the ac field) allowed by the Pauli principle:

$$|\Phi_{1,\ldots,N}(t=0)\rangle$$
$$=\hat{\mathbf{A}}\{|\Psi_{n_1\ell_1}(1)\rangle\otimes|\Psi_{n_2\ell_2}(2)\rangle\cdots\otimes|\Psi_{n_N\ell_N}(N)\rangle\}. \tag{30}$$

The one-period time-evolution operator for the N-electron system is given by the tensor product,

$$\boldsymbol{U}=U_1(1,0)\otimes U_2(1,0)\cdots\otimes U_N(1,0). \tag{31}$$

Since the antisymmetrization and time-evolution operators commute, the state after N_T periods is simply given by

$$|\Phi_{1,\ldots,N}(N_T)\rangle=\boldsymbol{U}^{N_T}|\Phi_{1,\ldots,N}(t=0)\rangle$$
$$=\hat{\mathbf{A}}\{U_1^{N_T}|\Psi_{n_1\ell_1}(1)\rangle\cdots\otimes U_N^{N_T}|\Psi_{n_N\ell_N}(N)\rangle\}, \tag{32}$$

where we have used the notation $U_i(1,0)\equiv U_i$, for $i=1,\ldots,N$. We can now generalize Eq. (29) for the trace of an operator at any integer multiple N_T of the period as

$$\mathrm{Tr}\{\hat{O}\}(t=N_T)=\langle\Phi_{1,\ldots,N}(t=N_T)|\hat{O}|\Phi_{1,\ldots,N}(t=N_T)\rangle$$
$$=\frac{1}{N}\sum_{i,j=1}^{N}\langle\Psi_{n_i\ell_i}(j,t=0)|(U_j^{\dagger})^{N_T}$$
$$\times\hat{O}_jU_j^{N_T}|\Psi_{n_i\ell_i}(j,t=0)\rangle. \tag{33}$$

In particular, for the average quantum time-dependent magnetization *per electron*, we have

$$\frac{\langle\tilde{M}_z\rangle(N_T)}{N}=-\frac{L}{N}+\frac{1}{N^2}\sum_{i,j=1}^{N}\langle\Psi_{n_i\ell_i}(j)|(U_j^{\dagger})^{N_T}$$
$$\times\left(-\frac{f}{2}r_j^2\right)U_j^{N_T}|\Psi_{n_i\ell_i}(j)\rangle, \tag{34}$$

where $L=\Sigma_{i=1}^{N}\ell_i$. Similarly, we can write the corresponding expressions for the time-dependent orbital currents, and the total time-dependent Hamiltonian average, which we term the averaged energy. For example, the *time-averaged magnetization* $\langle\langle M_z\rangle\rangle$ is defined by

$$\langle\langle M_z\rangle\rangle=\lim_{N_T\to\infty}\frac{1}{N_T}\sum_{n=1}^{N_T}\langle M_z\rangle(n). \tag{35}$$

III. RESULTS

We now come to the discussion of the main results of this paper, that are concerned with the dynamic and time-averaged properties of different relevant operators. The most striking features are observed in the magnetization of the system, which we shall discuss first as a function of the number N of electrons and $(\epsilon,\tilde{\omega}_c)$. We also give results for the orbital current as well as interesting results for the time-averaged energy as a function of N in different $(\epsilon,\tilde{\omega}_c)$ parameter regimes.

A. Magnetization, orbital currents, and energy

We start with the time-dependent dynamics of the magnetization and its corresponding power spectra for a single electron. The power spectrum $S(\nu)$ is the square of the Fourier transform of the expectation value of the magnetization operator $\langle\tilde{M}_z\rangle(t)$. [For notational simplicity, we write $\langle\tilde{M}_z\rangle(t)$ by $\langle M\rangle(t)$.] We keep $\tilde{\omega}_c$ fixed, and sweep through values of ϵ, from small to large. As can be seen from the

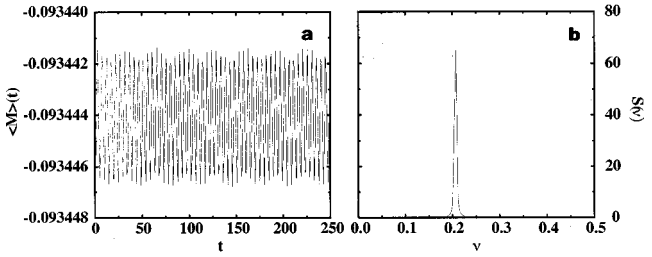

FIG. 2. (a) Single electron time-dependent magnetization $\langle M\rangle(t)$ for $\epsilon=0.1$, $\tilde{\omega}_c=0.1$, and $\tilde{\hbar}=0.1$ in the quasiregular regime (see Fig. 1). (b) Power spectrum, $S(\nu)$, of $\langle M\rangle$ corresponding to the parameter values of (a). The scale of ν frequencies is arbitrary. In all figures the axes are given in terms of dimensionless units.

phase diagram in Fig. 1, for fixed $\tilde{\omega}_c$, as ϵ increases the underlying classical dynamics changes from quasi-integrable to chaotic.

In Fig. 2(a) we see that $\langle M\rangle$ is diamagnetic in the regular regime and oscillates periodically with time, reflected in the very strong peak in its power spectrum shown in Fig. 2(b). As we increase the values of ϵ (i.e., as we approach the chaos border in the phase diagram), the intermediate dynamics gets more complex, as shown in Figs. 3(a) and 3(b). We see in Fig. 3(b), that there are two peaks in $S(\nu)$, which are due to the quasibeats seen in Fig. 3(a). In the chaotic region, $\langle M\rangle(t)$ shows essentially irregular behavior, Fig. 4(a), while $S(\nu)$ has a broad background, shown in Fig. 4(b). Note that the average value of $\langle M\rangle(t)$ increases in magnitude, becoming steadily more diamagnetic in the chaotic regime.

The one-electron behavior changes significantly with the addition of more electrons. The pattern of change from regular to chaotic is similar as in the one-electron case as we sweep through the same ϵ values as above. The spectral function develops more resonances in the regular region, whereas in the chaotic regime it has a broadband spectrum. As we continue to increase the number of electrons there are more ''beats'' in the time dependence of the magnetization and more peaks in the spectral function.

It is then more convenient to consider the time-averaged properties of the magnetization, the orbital current, or the total energy, as a function of the number of electrons. It is in this type of function that we can see important qualitative differences that represent the changes from the classical regular to chaotic behavior in the quantum dynamics. In Fig. 5(a) we see that for two electrons the time-averaged magnetization in the regular regime is *paramagnetic*, whereas for three electrons becomes diamagnetic again. We note that the diamagnetic to paramagnetic changes are nonmonotonic as a function of N. For example, for $N=4$ it switches back to paramagnetic, but remains diamagnetic for both $N=5$ and $N=6$. A similar situation occurs with the orbital current as shown in Fig. 5(b). We mention that the specific value of the frustration parameter ($f=\tilde{\omega}_c/\tilde{\hbar}$) determines if the magnetization flips from diamagnetic to paramagnetic as we keep adding electrons. Basically, this phenomenon occurs when $f\sim O(1)$, i.e., when we add one flux quantum to the dot. In all other cases, the magnetization remains diamagnetic and monotonically increasing in magnitude as the number of

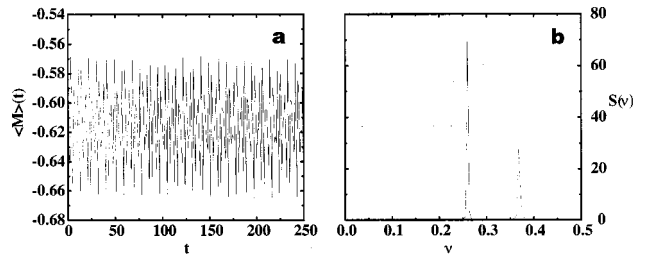

FIG. 3. (a) Same as in Fig. 2(a) for $\epsilon=1.0$, $\tilde{\omega}_c=1.0$, $\tilde{\hbar}=0.1$, which is in the regime that is approaching the chaotic region in parameter space (see Fig. 1). (b) Same as in Fig. 2(b) for the parameters of (a).

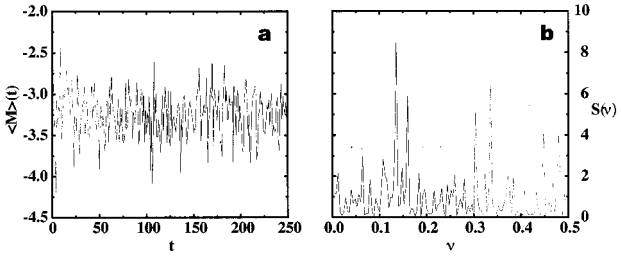

FIG. 4. (a) Magnetization as a function of time for the parameters $\epsilon=2.0$, $\tilde{\omega}_c=2.0$, and $\tilde{\hbar}=0.1$, deep in the chaotic regime (see Fig. 1). (b) Here the classical chaos is clearly revealed in the noisy structure of $\langle M\rangle$ and the broadband spectrum of $S(\nu)$.

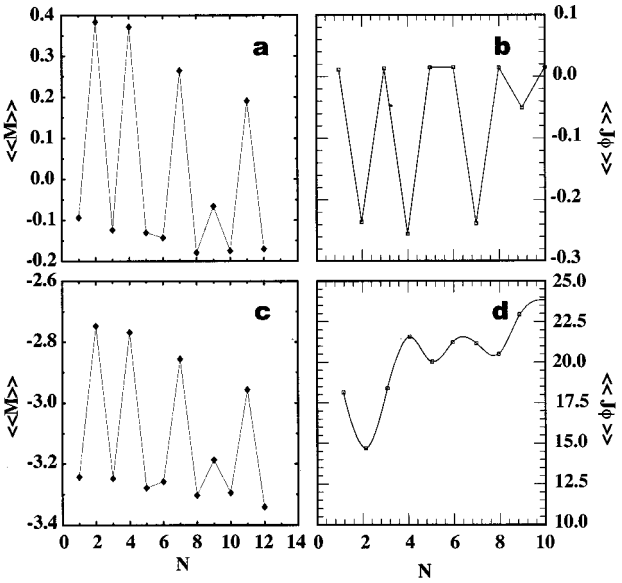

FIG. 5. (a) Time-averaged magnetization $\langle\langle M\rangle\rangle$ (per electron) in the quasi-integrable regime for $\epsilon=0.1$, $\tilde{\omega}_c=0.1$, $\tilde{\hbar}=0.1$, as a function of electron number N. We see that $\langle\langle M\rangle\rangle$ oscillates nonmonotonically with N. See the text for a theoretical perturbative explanation of these oscillations. (b) Total time-averaged orbital magnetization (per electron) as a function of N for the same parameter values as in (a). Here we see, as expected, a direct correspondence with the magnetization of (a). (c) Same as in (a) for parameters in the chaotic regime, $\epsilon=2.0$, $\tilde{\omega}_c=2.0$, and $\tilde{\hbar}=0.1$. In this case $\langle\langle M\rangle\rangle$ oscillates but its behavior is *purely* diamagnetic. (d) Orbital current for the chaotic parameter values of (c), with a clear correspondence to the purely diamagnetic nature of the magnetic response of the system in the chaotic regime.

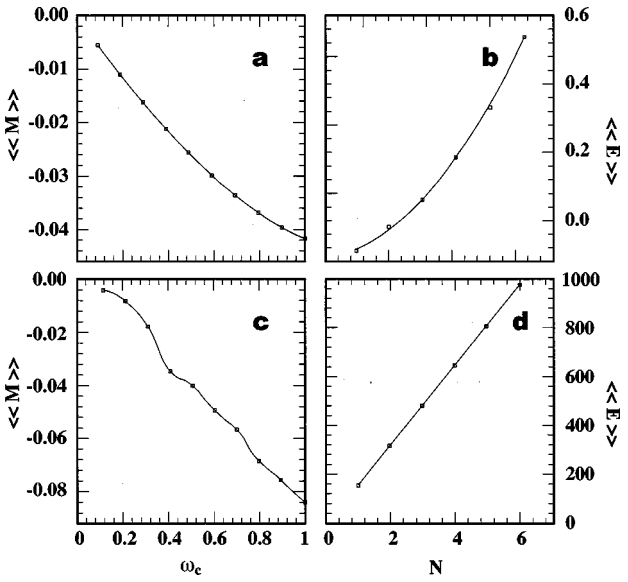

FIG. 6. (a) Time-averaged magnetization for one electron as a function of $\tilde{\omega}_c$ for $\epsilon=0.1$, and $\tilde{\hbar}=0.1$, with increment in diamagnetism as $\tilde{\omega}_c$ increases. (b) Time-averaged energy as a function of electron number with a clear quadratic dependence for the same parameters as in (a). (c) $\langle\langle M\rangle\rangle$ in the chaotic regime for one electron, with $\epsilon=10$, $\tilde{\hbar}=0.1$, as a function of $\tilde{\omega}_c$. Here we also note an increase of diamagnetism as $\tilde{\omega}_c$ grows. (d) $\langle\langle E\rangle\rangle$ for the same parameters as in (b) in the chaotic regime with a clear linear dependence on N. See the text for a further discussion of these results.

electrons increases. We provide a theoretical perturbation theory explanation of these diamagnetic to paramagnetic transitions results in the next subsection.

As we increase the value of ϵ, we enter the chaotic regime. There we find that for *all* electron numbers the magnetization is *always diamagnetic*, at least up to the maximum number of electrons we considered (~ 25). In Fig. 5(c) we show the time-averaged magnetization in the chaotic regime, which also oscillates as a function of N, but it is always negative and of larger magnitude than in the quasiregular regime. A similar situation occurs for the orbital current [as shown in Fig. 5(d), although it has less sharp changes as a function of N than does $\langle\langle M\rangle\rangle$].

In Fig. 6(a) we consider the time-averaged magnetization for a fixed value of $N=1$, $\epsilon=0.1$ and $\tilde{\hbar}=0.1$ as a function of ω_c. In this quasi-integrable regime we see that $\langle\langle M\rangle\rangle$ is diamagnetic and decays quadratically as a function of ω_c. The situation changes in the chaotic regime, shown in Fig. 6(c), where there is also decay with ω_c but now the behavior is not as smooth as in the quasi-integrable regime. We show in Fig. 6(b) the behavior of the time averaged energy as a function of the number N of electrons. Here we see a clear quadratic growth as a function of N. The situation is remarkably different when the single-particle classical dynamics is chaotic. In this case, shown in Fig. 6(d), the time-averaged energy grows clearly *linearly* with N. This implies that the classically chaotic solutions do have a significant quantum signature in the averaged energy, that changes the quadratic quasi-integrable regime behavior to a linear N dependence in the chaotic regime. We now present a simple heuristic argument as to why the change over between quadratic and linear N behavior is actually directly related to the Pauli exclusion principle. We note that in the zero magnetic field case, each of the N electrons in the circular dot of radius R_0 occupies an exclusion principle space of order $R_0/N^{1/2}$, while the static free particle kinetic energy changes as N/R_0^2. We expect that this situation does not change much when we are in the quasi-integrable regime, for finite fields and low frequencies. In the classically chaotic regime, in the presence of stronger magnetic fields or higher frequencies, the magnetic field will tend, on the average, to localize more the electrons to Larmor orbits inside the dot and in the boundaries. When the field is larger, so that the Larmor radius and R_0 are comparable, the Landau levels have to be taken into account. In this case the electrons will not necessarily feel the presence of the boundary and they will remain localized in their ''chaotic'' Landau orbits due to the time-dependent kicks. In this limit the contribution from the kinetic energy is much less relevant, and the Larmor orbit radius will be less dependent of N and R_0.

B. Perturbative evaluation of the magnetization in the quasiregular regime

In this subsection we present a perturbative analysis that provides an explanation for the magnetization oscillations as a function of N in the quasi-integrable regime. Let us first consider the time-independent part of the one-electron Hamiltonian $\tilde{H}$, and write it as

$$\tilde{H}_{\rm dc}=\tilde{H}_0+\tilde{V}, \tag{36}$$

where

$$\tilde{H}_0=-\frac{\tilde{\hbar}^2}{2}\left(\frac{d^2}{dr^2}+\frac{1}{r}\frac{d}{dr}\right)+\frac{\ell^2\tilde{\hbar}^2}{2r^2}+\ell\tilde{\hbar}\frac{\tilde{\omega}_c}{2} \tag{37}$$

and

$$\tilde{V}=\frac{1}{2}\left(\frac{\tilde{\omega}_c}{2}\right)^2 r^2. \tag{38}$$

We will consider the limiting case of very small $B_{\rm dc}$ field, i.e., $\tilde{\omega}_c \ll 1$. As was first shown by Dingle, one can write the eigenvalues to first order in $\tilde{\omega}_c$, by considering the zero field basis functions of the disk Bessel eigenfunctions

$$\tilde{H}_0|\psi_{n\ell}^{(1)}\rangle \simeq E_{n\ell}^{(1)}|\psi_{n\ell}^{(1)}\rangle, \tag{39}$$

where the normalized eigenvalues are [3]

$$E_{n\ell}^{(1)}=\frac{\alpha_{n\ell}^2}{2f}+\ell+\frac{f}{12}\left\{1+\frac{2(\ell^2-1)}{\alpha_{n\ell}^2}\right\}+O(\tilde{\omega}_c^2). \tag{40}$$

Here $\alpha_{n\ell}$ is the nth zero of the Bessel function $J_\ell(x)$, and the *unperturbed* basis functions are given by (we consider only the radial part, the angular part is clear)

$$\langle r|\psi_{n\ell}^{(0)}\rangle=\frac{\sqrt{2}}{J_{\ell+1}(\alpha_{n\ell})}J_\ell(\alpha_{n\ell}r). \tag{41}$$

The matrix elements of the perturbation are then given by

$$\langle \psi^{(0)}_{m\ell}|\tilde{V}|\psi^{(0)}_{n\ell}\rangle \equiv \tilde{V}_{mn} = \frac{1}{2}\left(\frac{\tilde{\omega}_c}{2}\right)^2 \begin{cases} \frac{1}{3}\left[1+\frac{2(\ell^2-1)}{\alpha^2_{n\ell}}\right], & m=ni \\ \frac{8\alpha_{m\ell}\alpha_{n\ell}}{(\alpha^2_{m\ell}-\alpha^2_{n\ell})^2}, & m\neq n. \end{cases} \tag{42}$$

The perturbed nondegenerate eigenfunctions are obtained from standard perturbation analysis,

$$|\psi^{(1)}_{n\ell}\rangle = |\psi^{(0)}_{n\ell}\rangle + \sum_{m\neq n}\frac{\tilde{V}_{mn}}{E^{(0)}_{m\ell}-E^{(0)}_{n\ell}}|\psi^{(0)}_{m\ell}\rangle + O(\tilde{V}^2_{mn})$$

$$= |\psi^{(0)}_{n\ell}\rangle + 2f\tilde{\omega}_c^2\sum_{m\neq n}\frac{\alpha_{m\ell}\alpha_{n\ell}}{(\alpha^2_{m\ell}-\alpha^2_{n\ell})^3}|\psi^{(0)}_{m\ell}\rangle + O(\alpha^{-8}), \tag{43}$$

where we have used the unperturbed energy levels $E^{(0)}_{m\ell}-E^{(0)}_{n\ell}=\frac{1}{4}(\alpha^2_{m\ell}-\alpha^2_{n\ell})$. Using Eq. (43), and the definition of the magnetization operator, Eq. (14), the leading first order matrix element contribution to $\tilde{M}_z$ is given by

$$\langle \psi^{(1)}_{n\ell}|\tilde{M}_z|\psi^{(1)}_{n\ell}\rangle \equiv \langle \tilde{M}_z\rangle_{mn} = -\ell - 2f\langle \psi^{(0)}_{n\ell}|r^2|\psi^{(0)}_{n\ell}\rangle + O(\tilde{\omega}_c^2) \tag{44}$$

$$= -\ell - \frac{2f}{3}\left[1+\frac{2(\ell^2-1)}{\alpha^2_{n\ell}}\right] + O(\tilde{\omega}_c^2). \tag{45}$$

Once again, if we take as the initial state the lowest energy state allowed by the Pauli principle

$$|\Psi_{1,\ldots,N}(0)\rangle = \hat{\mathbf{A}}\{|\psi_{n_1\ell_1}(1)\rangle\otimes|\psi_{n_2\ell_2}(2)\rangle\cdots \otimes|\psi_{n_N\ell_N}(N)\rangle\}, \tag{46}$$

we can generalize Eq. (44) to the N-electron case. We find that the averaged magnetization *per electron*, to first order approximation, is

$$\frac{\langle \tilde{M}_z\rangle}{N} = -\frac{2f}{3} - \frac{1}{N}\sum_{i=1}^{N}\left\{\ell_i + \frac{4f}{3}\frac{(\ell_i^2-1)}{\alpha^2_{n_i\ell_i}}\right\} + O(\tilde{\omega}_c^2). \tag{47}$$

Next, we perform a linear-response theory analysis of the *full* time-dependent problem, assuming that $\epsilon \ll 1$. We show in the Appendix that within the perturbative approximation for a single electron, the average magnetization at time N_T is given by

$$\langle \tilde{M}_z\rangle(N_T) \simeq -\left\{\ell_i + \frac{f}{2}\langle r^2\rangle_{n_i,n_i}\right\} + \frac{f}{2\tilde{\hbar}}\left(\frac{\epsilon\tilde{\omega}_c}{2}\right)^2 \times \sum_{p=1}^{N_T}\sum_{n\neq n_i}\langle r^2\rangle^2_{n,n_i}\sin\{\omega_{n_i,n}(N_T-p)\}, \tag{48}$$

where

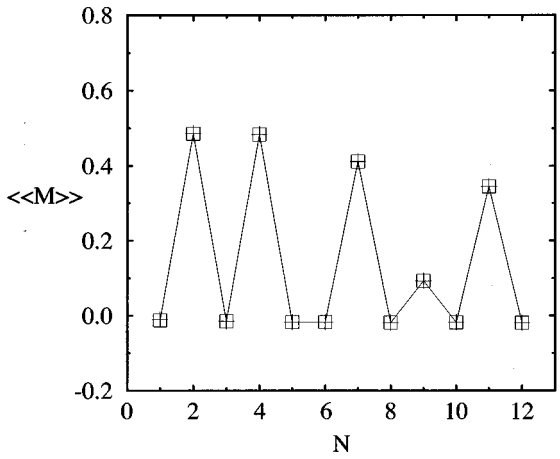

FIG. 7. Comparison between exact (□) and perturbative (+) calculations for the time-averaged magnetization as a function of electron number. The parameters here are $\epsilon=0.01$, $\tilde{\hbar}=0.1$, and $\tilde{\omega}_c=0.01$. Note the almost exact agreement between the two calculations, with the magnitude of the diamagnetic response much smaller than that of the paramagnetic response.

$$\langle r^2\rangle_{n,n_i} = \frac{1}{3}\left[1+\frac{2(\ell_i^2-1)}{\alpha^2_{n_i\ell_i}}\right] + O(\tilde{\omega}_c^2). \tag{49}$$

Clearly, the last term in Eq. (48) is of $O(\tilde{\omega}_c^3)$, so it can be ignored within the current approximation, which means that to lowest order, the time dependence plays no significant role in determining the average magnetization.

To test the approximation for $\langle \tilde{M}_z\rangle/N$, Eq. (47), we show in Fig. 7 a comparison of results from the perturbative and numerically exact calculations. The perturbative results agree remarkably well with the numerical calculations. We can now understand why the averaged magnetization oscillates in sign in the regular regime, and it is because $\langle \tilde{M}_z\rangle/N$ depends most strongly on $\Sigma_{i=1}^N \ell_i$. Whenever this sum of angular momentum quantum numbers flips sign, so does the magnetization. For example, for the parameters shown in Fig. 7, the values of $F(N)=\Sigma_{i=1}^N \ell_i$ for successive values of N are

$$F(N=1,2,\ldots,12) = 0,-1,0,-2,0,0,-3,0,-1,0,-4,0, \tag{50}$$

corresponding to

$$\ell_i = (0,-1,1,-2,2,0,-3,3,-1,1,-4,4), \tag{51}$$

i.e., the ℓ values of the twelve-electron (unperturbed) ground state. This is a selection rule associated with the symmetries present in the system.

What is interesting is that in the chaotic region, there is no such flipping of the sign. This difference may constitute an experimentally accessible signature of chaos in the quantum system. Clearly, such behavior is exclusively a consequence of the Pauli principle, for we would not observe any change in the response per electron without it, since ignoring it in the multielectron case would lead to a trivial rescaling of the single electron results.

IV. CONCLUSIONS

To summarize, we have studied a model of a noninteracting N-electron system, confined to a circular structure with rigid boundaries, and subjected to perpendicular constant and time-periodic magnetic fields. We studied the magnetization and orbital currents as a function of time, as well as the time-averaged magnetization $\langle\langle \tilde{M}_z \rangle\rangle$, and energy as a function of electron number N. We can make a strong connection between the dynamic response of $\langle \tilde{M}_z \rangle(t)$ (or it's power spectrum), and the underlying classical dynamics—as the classical system makes a transition to chaos as we vary the applied magnetic fields, the dynamics changes from being harmonic to essentially noisy. There are three central significant conclusions: first, the Pauli principle affects the behavior of this noninteracting system significantly, e.g., in terms of oscillations of $\langle\langle \tilde{M}_z \rangle\rangle$ as a function of N. This behavior is directly related to the Pauli principle that allows the electrons to optimally reduce their averaged $\langle\langle M \rangle\rangle$ at specific values of the total angular momentum. Second, while these oscillations in the quasi-integrable regime cause the system to flip back and forth between diamagnetic and paramagnetic behavior, the system remains diamagnetic at all times in the chaotic regime. We also found a very interesting change in the time-averaged energy as a function of N, going from quadratic in the quasi-integrable regime to linear in the chaotic one. We provided a simple heuristic explanation of this behavior related to Pauli's exclusion principle.

In this paper we have not considered the effects of Coulomb interactions that can significantly complicate the analyses. There are static studies that have considered the changes in the classical dynamics due to interactions. What has been found in some examples is that if the system of noninteracting particles was nonchaotic, as the interaction parameter increases the dynamics can become chaotic [23]. In the quantum regime the random matrix theory statistics can exhibit a transition from Poisson to orthogonal ensemble as the interaction strength increases [24]. What happens in the time-dependent case considered in this paper that deals with quasienergy statistics is not known at present.

Here we have considered a circular disk in the presence of a time dependent magnetic field. It is only when we have the ac component of the field added to the dc one that chaos appears. In contrast, if the field is static but the geometry is changed one can have chaotic classical solutions. The relevance of the Pauli principle as seen in the zero temperature magnetization has been studied, for example, by Ref. [5]. At present we do not know what happens when the geometry is not circular and we have a gas of Pauli electrons in the presence of a dc+ac magnetic field. We expect to consider the two problems mentioned above in the future.

To conclude, we briefly give some estimates in terms of physical units of the field strengths and frequencies required to observe the effects predicted by our model calculations. In a GaAs-AlGaAs semiconductor the radius R_0 of a quantum dot device [10–18] can be between 0.1 and 10 μm, a sheet electron density $n \sim 10^{11}$ cm^{-2}, a mobility $\mu \sim 265\,000$ cm^2/V s, and a characteristic level spacing $\Delta\epsilon \sim 0.05$ meV or ~ 0.5 K. In the ballistic electronic motion regime the elastic mean free path $l_\phi \sim 10$ μm, with phase coherence length varying between 15 and 50 μm. Typically the power injected is smaller than 1 nW, which is necessary to avoid electron heating. For a dot radius of $R_0 \sim 1$ μm, the kick frequency ω_0 can be obtained from Eqs. (5) as $\omega_0 = (\hbar/m^* R_0^2)\,(1/\tilde{\hbar}) \simeq 2/\tilde{\hbar}$ GHz. Then the required $B_{\rm dc}$ and $B_{\rm ac}$ magnetic fields have the values $B_{\rm dc} = (\omega_0 m^* c/e^*)\,\tilde{\omega}_c \simeq 20(\tilde{\omega}_c/\tilde{\hbar})$ G, and $B_{\rm ac} = \epsilon B_{\rm dc} \simeq 20(\epsilon\tilde{\omega}_c/\tilde{\hbar})$ G. The ac Larmor frequency is $\omega_{\rm ac} = \epsilon\tilde{\omega}_c \simeq 20\,(\epsilon\tilde{\omega}_c/\tilde{\hbar})$ MHz. With these values, in the quasi-integrable regime, with parameters $(\epsilon, \tilde{\omega}_c)^{(\rm reg)} = (0.1, 0.1)$, we get $\omega_0^{(\rm reg)} \simeq 20$ GHz and $B_{\rm ac}^{(\rm reg)} \simeq 20$ G. In the chaotic regime we take the parameters $(\epsilon, \tilde{\omega}_c)^{(\rm chaos)} = (2.0, 2.0)$, which leads to $\omega_0^{(\rm chaos)} \simeq 20$ GHz and $B_{\rm ac}^{(\rm chaos)} \simeq 800$ G. These results for the regular and chaotic regimes are within experimental reach.

ACKNOWLEDGMENTS

This work has been supported in part by CONACYT 3047P and by NSF Grant No. DMR-9521845.

APPENDIX

In this Appendix we provide the derivation of Eq. (48). For any operator $\hat{A}$, the expectation value of the linear response under the action of a constant Hamiltonian H_0 and a time-dependent perturbation $V(t)$ is given by

$$\langle \hat{A} \rangle(t) = \langle \hat{A} \rangle_0 + \frac{1}{i\hbar} \int_0^t dt_1 \langle [\hat{A}(t_1 - t), \hat{V}(t_1)] \rangle_0 , \tag{A1}$$

where $\langle \cdots \rangle_0 = \mathrm{Tr}\{\rho_0\}$, and ρ_0 is the density matrix associated with the unperturbed Hamiltonian H_0. Thus,

$$\langle [\hat{A}(t_1 - t), \hat{V}(t_1)] \rangle_0 = \mathrm{Tr}\{\rho_0 [\hat{A}(t_1 - t), \hat{V}(t_1)]\} = \mathrm{Tr}\{\rho_0 e^{iH_0(t_1-t)/\hbar} \hat{A} e^{-iH_0(t_1-t)/\hbar} \hat{V}(t_1) - \rho_0 \hat{V}(t_1) e^{iH_0(t_1-t)/\hbar} \hat{A} e^{-iH_0(t_1-t)/\hbar}\}. \tag{A2}$$

For a single particle pure state $|\psi_{n_i}\rangle$, $\rho_0 = |\psi_{n_i}\rangle\langle\psi_{n_i}|$. Thus, from above,

$$\langle\cdots\rangle_0=\sum_n \langle\psi_n|\psi_{n_i}\rangle\langle\psi_{n_i}|e^{iH_0(t_1-t)/\hbar}\hat{A}e^{-iH_0(t_1-t)/\hbar}V(t_1)|\psi_n\rangle-\sum_n \langle\psi_n|\psi_{n_i}\rangle\langle\psi_{n_i}|\hat{V}(t_1)e^{iH_0(t_1-t)/\hbar}\hat{A}e^{-iH_0(t_1-t)/\hbar}|\psi_n\rangle$$
$$=e^{iE_{n_i}(t_1-t)/\hbar}\langle\psi_{n_i}|\hat{A}e^{-iH_0(t_1-t)/\hbar}\hat{V}(t_1)|\psi_{n_i}\rangle-e^{-iE_{n_i}(t_1-t)/\hbar}\langle\psi_{n_i}|\hat{V}(t_1)e^{-iH_0(t_1-t)/\hbar}\hat{A}|\psi_{n_i}\rangle$$
$$=e^{iE_{n_i}(t_1-t)/\hbar}\sum_n e^{-iE_{n_i}(t_1-t)/\hbar}\langle\psi_{n_i}|\hat{A}|\psi_n\rangle\langle\psi_n|\hat{V}(t_1)|\psi_{n_i}\rangle-e^{-iE_{n_i}(t_1-t)/\hbar}\sum_n e^{iE_{n_i}(t_1-t)/\hbar}\langle\psi_{n_i}|\hat{V}(t_1)|\psi_n\rangle\langle\psi_n|\hat{A}|\psi_{n_i}\rangle. \tag{A3}$$

In our case,

$$\hat{A}=\tilde{M}_z=-\frac{\hat{L}_z}{\tilde{\hbar}}-\frac{f}{2}\hat{r}^2,$$

$$\hat{V}(t_1)=\tilde{V}\sum_{p=0}^{N_T}\delta(t_1-p). \tag{A4}$$

Since the $\{|\psi_n\rangle\}$ are real and $\hat{A}$ and $\hat{V}$ are Hermitian,

$$\langle\cdots\rangle_0=\sum_n A_{n_i,n}V_{n,n_i}(t_1)(e^{i\omega_{n_i,n}(t_1-t)}-e^{-i\omega_{n_i,n}(t_1-t)}), \tag{A5}$$

where

$$A_{n_i,n}=-\mathscr{l}_i\delta_{n_i,n}-\frac{f}{2}\langle\psi_{n_i}|r^2|\psi_n\rangle\equiv-\mathscr{l}_i\delta_{n_i,n}-\frac{f}{2}\langle r^2\rangle_{n_i,n}, \tag{A6}$$

$$V_{n,n_i}=\frac{1}{2}\left(\frac{\epsilon\tilde{\omega}_c}{2}\right)^2\langle r^2\rangle_{n,n_i}\sum_p \delta(t_1-p), \tag{A7}$$

$$\omega_{n_i,n}=\frac{E_{n_i}-E_n}{\tilde{\hbar}}. \tag{A8}$$

Finally, we have

$$\langle\ldots\rangle_0=-i\left(\frac{\epsilon\tilde{\omega}_c}{2}\right)^2\sum_n \langle r^2\rangle_{n,n_i}\left(\mathscr{l}_i\delta_{n_i,n}+\frac{f}{2}\langle r^2\rangle_{n,n_i}\right)\sum_{p=0}^{N_T}\sin\{\omega_{n_i,n}(t_1-t)\}\delta(t_1-p) \tag{A9}$$

and

$$\langle A\rangle_0=\langle\psi_{n_i}|\tilde{M}_z|\psi_{n_i}\rangle=-\mathscr{l}_i-\frac{f}{2}\langle r^2\rangle_{n_i,n_i}. \tag{A10}$$

Substituting Eqs. (A9) and (A10) into Eq. (A1), we get Eq. (48). This completes our derivation of the linear response result.

[1] J. H. Van Leeuwen, J. Phys. (Paris) **2**, 361 (1921); J. H. Van Vleck, Proc. Natl. Acad. Sci. USA **14**, 178 (1928).

[2] L. Landau and V. Fock, Z. Phys. **47**, 446 (1928); **64**, 629 (1930).

[3] R. B. Dingle, Proc. R. Soc. London, Ser. A **211**, 500 (1952); **212**, 47 (1952).

[4] For recent reviews, see T. Chakraborty, Comments Condens. Matter Phys. **16**, 35 (1992); M. A. Kastner, Phys. Today **46** (1), 24 (1993); D. Heitmann and J. Kotthaus, *ibid.* **46** (6), 56 (1993); N. F. Johnson, J. Phys.: Condens. Matter **7**, 965 (1995); M. A. Kastner, Comments Condens. Matter Phys. **17**, 349 (1996); R. C. Ashori, Nature (London) **379**, 413 (1996); J. H. Jefferson and W. Häusler, Mol. Phys. Rep. **17**, 81 (1997); L. Jacak, P. Hawrylak, and A. Wójs, *Quantum Dots* (Springer, Berlin, 1998); L. P. Kouwenhouven, T. H. Osterkamp, M. W. S. Danoesastro, M. Eto, D. G. Austing, T. Honda, and S. Tarucha, Science **278**, 1788 (1997); N. B. Zhitenev, R. C. Ashoori, L. N. Pfeiffer, and K. W. West, Phys. Rev. Lett. **79**,

2308 (1997); P. L. McEuen, N. S. Wingreen, E. B. Foxman, J. Kinaret, U. Meirav, M. A. Kastner, and Y. Meir, Physica B **189**, 70 (1993).
[5] K. Nakamura and H. Thomas, Phys. Rev. Lett. **61**, 247 (1988).
[6] U. Sivan and Y. Imry, Phys. Rev. Lett. **61**, 1001 (1988).
[7] Yigal Meir, O. Entin-Wohlman, and Yuval Gefen, Phys. Rev. B **42**, 8351 (1990).
[8] S. Oh, A. Yu. Zyuzin, and R. A. Serota, Phys. Rev. B **44**, 8858 (1991); Y. H. Zeng, B. Goodman, and R. A. Serota, *ibid.* **47**, 15 660 (1993).
[9] P. A. Maksym and T. Chakraborty, Phys. Rev. Lett. **65**, 108 (1990); Phys. Rev. B **45**, 1947 (1992); P. A. Maksym, Physica B **184**, 385 (1993).
[10] C. M. Marcus *et al.*, Phys. Rev. Lett. **69**, 506 (1992).
[11] B. W. Alphenaar *et al.*, Phys. Rev. B **46**, 7236 (1992).
[12] R. P. Taylor *et al.*, Phys. Rev. Lett. **69**, 1989 (1992).
[13] A. T. Johnson *et al.*, Phys. Rev. Lett. **69**, 1592 (1992).
[14] M. Robnik and M. V. Berry, J. Phys. A **18**, 1361 (1985).
[15] D. Ullmo, K. Richter, and R. A. Jalabert, Phys. Rev. Lett. **74**, 383 (1995).
[16] O. Meplan, F. Brut, and C. Gignoux, J. Phys. A **26**, 237 (1993).
[17] U. Meirav, M. A. Kastner, and S. J. Wind, Phys. Rev. Lett. **65**, 771 (1990); M. A. Kastner, Rev. Mod. Phys. **64**, 849 (1992).
[18] L. P. Lévy, D. H. Reich, L. Pfeiffer, and K. West, Physica B **189**, 204 (1993).
[19] Y. Noat, H. Bouchiat, B. Reulet, and D. Mailly, Phys. Rev. Lett. **80**, 4995 (1998); B. Reulet, M. Ramin, H. Bouchiat, and D. Mailly, *ibid.* **75**, 124 (1995).
[20] R. Badrinarayanan and J. V. José, Phys. Rev. E **54**, 2419 (1996).
[21] C. W. J. Benakker and H. van Houten, Solid State Phys. **44**, 1 (1991).
[22] See, e.g., Kerson Huang, *Statistical Mechanics*, 2nd ed. (Wiley, New York, 1982).
[23] See, for example, D. Ullmo *et al.*, Phys. Rev. Lett. **80**, 895 (1998).
[24] See, for example, M. Pascaud and G. Montambaux, Ann. Phys. (Leipzig) **B7**, 406 (1998).